Inorganic Chemistry

Article

pubs.acs.org/IC

Synthesis and Structure of Dirhodium Analogue of Octaborane-12 and Decaborane-14

Dipak Kumar Roy, Shubhankar Kumar Bose, R. S. Anju, V. Ramkumar, and Sundargopal Ghosh*

Department of Chemistry, Indian Institute of Technology Madras, Chennai 600 036, India

Supporting Information

ABSTRACT: We present the results of our investigation of a thermally driven cluster expansion of rhodaborane systems with BH_3·THF. Four novel rhodaborane clusters, for example, *nido*-$[(Cp^*Rh)_2B_6H_{10}]$, **1**; *nido*-$[(Cp^*Rh)B_9H_{13}]$, **2**; *nido*-$[(Cp^*Rh)_2B_8H_{12}]$, **3**; and *nido*-$[(Cp^*Rh)_3B_8H_9(OH)_3]$, **4** (Cp^* = η^5-C_5Me_5), have been isolated from the thermolysis of $[Cp^*RhCl_2]_2$ and borane reagents in modest yields. Rhodaborane **1** has a *nido* geometry and is isostructural with $[B_8H_{12}]$. The low temperature ^{11}B and ^1H NMR data demonstrate that compound **1** exists in two isomeric forms. The framework geometry of **2** and **3** is similar to that of $[B_{10}H_{14}]$ with one BH group in **2** (3-position), and two BH groups in **3** (3, 4-positions) are replaced by an isolobal $\{Cp^*Rh\}$ fragment. The 11 vertex cluster **4** has a *nido* structure based on the 12 vertex icosahedron, having three rhodium and eight boron atoms. In addition, the reaction of rhodaborane **1** with $[Fe_2(CO)_9]$ yielded a condensed cluster $[(Cp^*Rh)_2\{Fe(CO)_3\}_2B_6H_{10}]$, **5**. The geometry of **5** consists of $[Fe_2B_2]$ tetrahedron and an open structure of $[(Cp^*Rh)_2B_6]$, fused through two boron atoms. The accuracy of these results in each case is established experimentally by spectroscopic characterization in solution and structure determinations in the solid state.

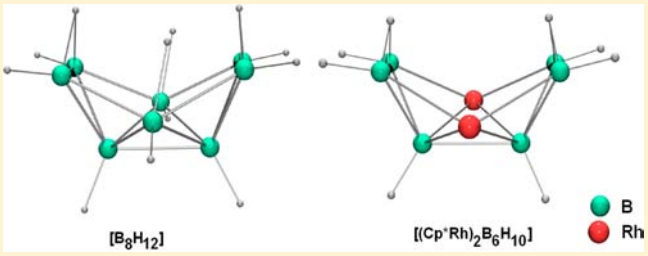

INTRODUCTION

The development of both cluster electron counting rules and the isolobal principle which flourished the development of metallaborane chemistry provide a solid foundation for understanding the interrelationships between structure and composition of cluster compounds.[1,2] The progress of metallaborane chemistry has emerged from several routes; however, the reaction of metal polychlorides and boranes are found out to be very fruitful for the synthesis of metallaborane compounds.[3] As a result, several metallaboranes of groups 5−9 have been synthesized which are prone to show different structural variety. For example, group 5 and 6 transition metals generally form stable $[M_2B_5H_{9+n}]$ (M = V, Ta, n = 2; M = Cr, Mo, W, n = 0).[4−8] In group 7, rhenium forms a series of *closo*-rhenaboranes with Re_2B_n framework (n = 4−10),[9] whereas in group 8, ruthenium offers interesting hydrogen rich open clusters.[10] Of the group 9 metals, in particular, iridium forms a number of clusters with open geometry.[11]

The recent development of metallaborane chemistry has focused on reactivity and structural properties. A dinuclear rhodaborane, $[(Cp^*Rh)_2B_3H_7]$, had shown its potentiality for the cyclotrimerization of both terminal and internal alkynes,[12] whereas a *nido*-hydridorhodathiaborane, [8,8,8-$(PPh_3)_2$(H)-9-(py)-*nido*-8,7-$RhSB_9H_9$], opens a door for catalytic hydrogenation of olefins.[13] Therefore, the chemistry of rhodaborane systems became of interest. Recently Fehlner et al. described a series of iridaboranes, from the thermally driven cluster expansion of *arachno*-$[\{Cp^*IrH_2\}B_3H_7]$ with $[BH_3$·THF$]$.[11] Thus, the existence of high nuclearity iridaborane clusters led us to investigate the rhodaborane system. In this Article, we present the results of the reaction between $[Cp^*RhCl_2]_2$ and monoboranes to afford four novel dirhodaboranes **1**−**4**. In addition, the chemistry of **1** with transition metal carbonyl compounds has been explored.

RESULTS AND DISCUSSION

Synthesis and Characterization of Rhodaboranes 1−4. As shown in Scheme 1, reaction of $[Cp^*RhCl_2]_2$ with 6-fold excess of $[LiBH_4$·THF$]$ followed by thermolysis in presence of excess $[BH_3$·THF$]$ at 105 °C yielded yellow **1**, colorless **2** and **3**, purple **4**, and known $[(Cp^*Rh)_3B_4H_4]$, **I**.[12] Although compounds **1**−**4** are produced in a mixture, these compounds can be separated by preparative thin-layer chromatography (TLC), allowing characterization of pure materials. Details of spectroscopic and structural characterization of compounds **1**−**4** are discussed below.

$[(Cp^*Rh)_2B_6H_{10}]$, 1. Compound **1** was isolated as a yellow, relatively air-stable solid in 20% yield. The IR spectrum of **1** features bands at 2498 and 2510 cm^{-1} owing to terminal B−H stretches. The ^{11}B NMR spectrum of **1** at room temperature shows two resonances at δ = 37.1 and 5.3 ppm in 2:1 ratio, indicating the presence of higher symmetry. Besides the BH terminal protons, two B−H−B and two Rh−H−B protons with an equal intensity were also observed in the ^1H NMR spectrum.

Received: May 22, 2012
Published: September 21, 2012

   dx.doi.org/10.1021/ic301070e | *Inorg. Chem.* 2012, 51, 10715−10722

Scheme 1. Synthesis of Rhodaboranes 1−4

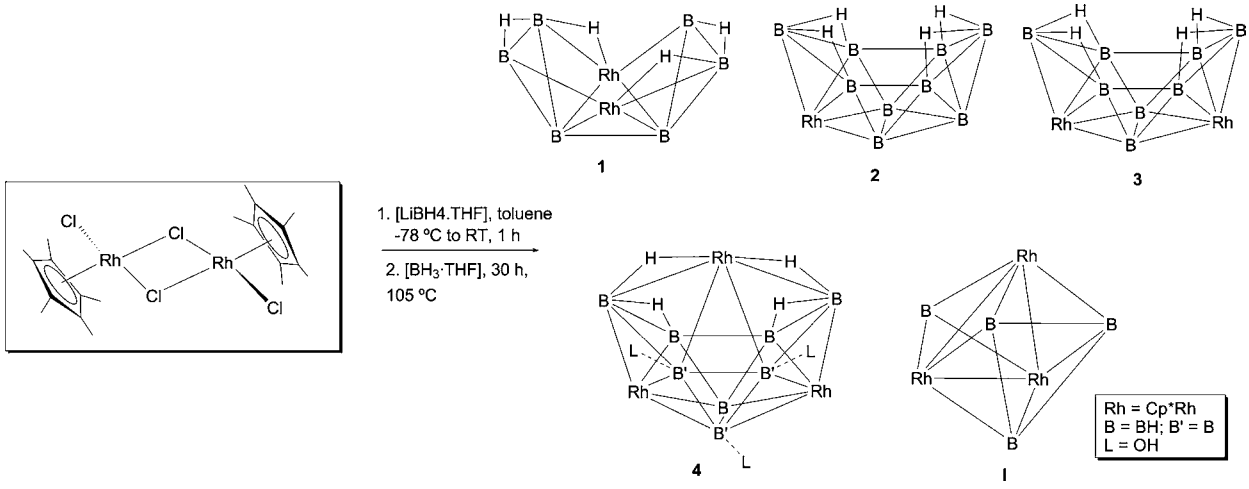

Furthermore, ^{1}H and ^{13}C NMR spectra imply 2 equiv of Cp* ligands consistent with its symmetrical structure.

In order to confirm the spectroscopic assignments and determine the crystal structure of **1**, an X-ray diffraction analysis was undertaken. As shown in Figure 1, the molecular structure

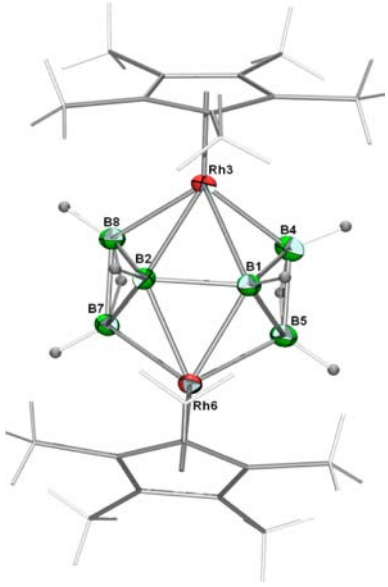

Figure 1. Molecular structure and labeling diagram for $[(Cp^*Rh)_2B_6H_{10}]$, **1**. Selected bond lengths (Å) and angles (deg): Rh6−B7 2.105(7), Rh6−B2 2.207(6), Rh6−B1 2.208(7), Rh3−B8 2.124(7), Rh3−B2 2.218(6), Rh3−B1 2.228(7), B1−B2 1.876(9), B7−B8 1.684(9), B2−B8 1.744(10), B4−B5 1.701(10); B7−Rh6−B5 100.9(3), B8−Rh3−B4 100.6(3), B7−B8−B2 60.9(4), B5−B1−B4 57.9(4), B4−B5−Rh6 120.6(5), Rh6−B1−Rh3 120.8(3).

of **1** can be viewed as a *nido* structure based on a *closo* tricapped trigonal prism with one vertex missing. The structure of **1** is similar to those of *nido*-$[B_8H_{12}]$,[14] *nido*-$[C_2B_6H_{10}]$,[15] and $[(Cp^*Ru)_2B_6H_{12}]$.[10] Considering {Cp*Rh} as a two-electron fragment, $[(Cp^*Rh)_2B_6H_{10}]$ possesses 10 skeleton electron pair (sep), consistent with the skeleton electron count of $[B_8H_{12}]$. The average Rh−B bond length of 2.17 Å is about 0.2 Å longer than observed for other rhodaboranes.[16] The B−B distances are in accord with the 8-vertex ruthenaborane $[(Cp^*Ru)_2B_6H_{12}]$.[10]

The CO ligand has been shown to undergo a smooth addition reaction with unsaturated five sep $[(Cp^*Cr)_2B_4H_8]$[17] and saturated six sep $[(Cp^*Re)_2B_4H_8]$[18] to yield corresponding saturated dimetallaboranes. As a result, we have examined the "obedient" nature of cluster **1** by performing the similar reaction with freshly prepared CO gas and transition metal carbonyl compounds. However, no sign of $[(Cp^*Rh)_2COB_6H_8]$ was observed even under more forcing conditions, and the investigation of the reaction of **1** with $[Co_2(CO)_8]$ gave disappointing results.

Solution Properties of 1. In a further attempt to confirm the assignment of hydrogen atoms of structure **1** (Scheme 1), a 2D $^{1}H\{^{11}B\}/^{11}B\{^{1}H\}$ HSQC experiment was performed. The HSQC experiment, shown in Figure 2, demonstrates that both

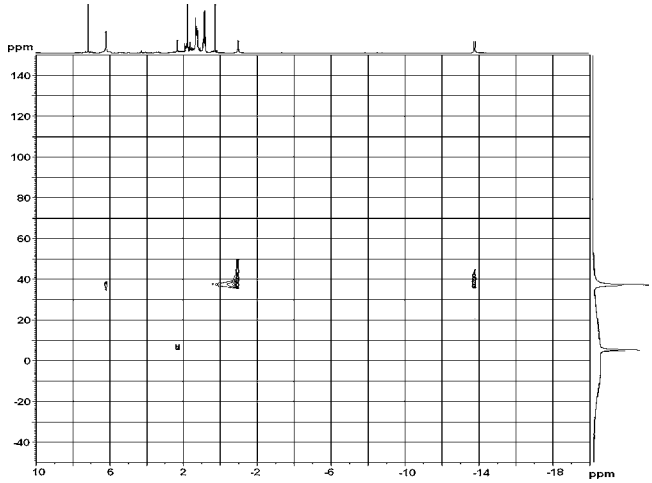

Figure 2. $^{1}H\{^{11}B\}/^{11}B\{^{1}H\}$ HSQC spectrum of **1**.

the Rh−H−B protons coupled exclusively to the boron atoms appearing at δ = 37.1 ppm and thus can be assigned to the open face boron atoms, and the B−H−B protons are also associated to the same open face boron atoms. The symmetric environment of $^{11}B\{^{1}H\}$ NMR spectrum and the HSQC experiments reveal that both the Rh−H−B hydrogen atoms are switching over the four open face boron atoms such as B4, B5, B7, and B8 (Figure 1).

To perceive the fluxionality of **1**, variable-temperature $^{1}H\{^{11}B\}$ and $^{11}B\{^{1}H\}$ NMR were undertaken. The high-field region of the $^{1}H\{^{11}B\}$ NMR, shown in Figure 3, sheds more

dx.doi.org/10.1021/ic301070e | Inorg. Chem. 2012, 51, 10715−10722

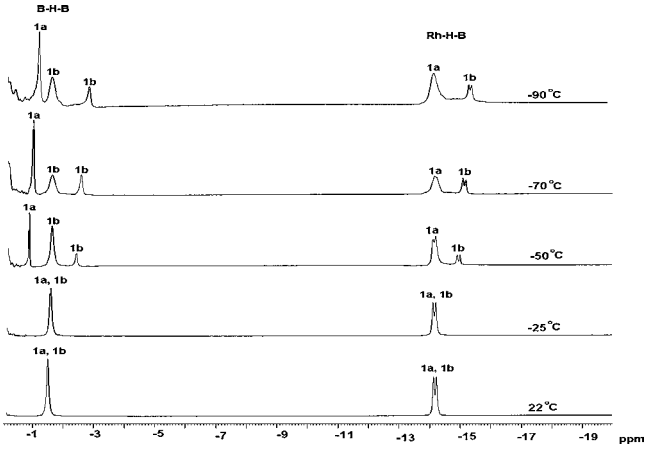

Figure 3. Variable-temperature $^{1}H\{^{11}B\}$ NMR spectrum of **1** in the hydride region showing that **1** exists as a mixture of two isomeric forms, **1a** and **1b**.

Chart 1. Interconversion of the Two Isomers of 1

1a **1b**

light into the structure of **1**. The outcome suggests the presence of two isomers (**1a** and **1b**, shown in Chart 1) which are undergoing rapid interconversion at room temperature on the NMR time scale. As the temperature is lowered, resonance at $\delta = -1.46$ ppm (B−H−B protons) splits into three distinct peaks at $\delta = -0.91$, -1.71, and -2.48 ppm. Similarly, the Rh−H−B protons at $\delta = -14.1$ ppm splits into two peaks at $\delta = -13.67$ and -14.92 ppm. Two resonances appearing at $\delta = -0.91$ and -13.67 ppm in a 1:1 ratio have been assigned to the B−H−B and Rh−H−B protons of **1a** isomer. Three resonances at $\delta = -1.71$, -2.48, and -14.92 ppm in a 1:1:2 ratio can be assigned to B−H−B, B−H−B, and Rh−H−B protons for **1b** isomer. These data allow us to identify the second species as a tautomer of **1a** and demonstrate the fluxional behavior of the molecule. The low temperature $^{11}B\{^{1}H\}$ NMR shows three resonances at $\delta = 37.1$, 5.3, and -20.2 ppm, which are comparable with **1a** isomer (Figure S1, Supporting Information, SI). To see further splitting in the $^{11}B\{^{1}H\}$ NMR for **1b**, we recorded ^{11}B NMR at -130 °C; however, not much information was obtained except broadening of individual resonances.

The structure of **1** is unusual and presents an interesting problem in the context of known structures of eight-atom clusters (Table S1, SI). As shown in Figure 4, **1** exhibits a cluster shape that can be derived from a nine vertex tricapped trigonal prism by removing one of the five-connect vertices followed by removal of one connection. Thus, it has *nido* geometry with 10 sep equal to the prescribed skeleton electron pair of 10. Similarly, $[B_8H_{12}]$ exhibits a geometry derived by removing a five connected vertex from tricapped trigonal prism. Hence, **1** has formal *nido* geometry and might also be classified as "normal".

$[(Cp^*Rh)B_9H_{13}]$, 2. Both compounds **2** and **3** are separated by careful preparative thin-layer chromatography on the laboratory bench with the aid of UV light. The spectroscopic data for compound **2** plus straightforward application of the electron counting rules generate a structure for the metal-laborane in solution, and it was confirmed by an X-ray structure in the solid state. The ^{11}B NMR shows six types of BH environments in 2:1:1:2:2:1 ratio that indicates the presence of a plane of symmetry with respect to the plane formed by Rh1, B2, B7, B8. All the boron atoms are connected to the terminal hydrogen atoms, and the extra bridging hydrogens are expected to be located on the open six-membered face. Furthermore, the ^{1}H NMR spectrum shows, in addition to the Cp* ligand and terminal B−H resonances, two distinct B−H−B groups in a ratio of 1:1. The ^{1}H NMR signal at $\delta = -3.85$ is assigned to the B−H−B in which boron atoms are connected to the metal.

On the basis of the electron counting rules, the framework geometry of **2** should be *nido*-$[(Cp^*Rh)B_9H_{13}]$ with a missing six connected vertex of a *closo* 11-vertex deltahedron (Figure 5). By analogy with the Co[19] and Ir[11] analogue, **2** can be considered

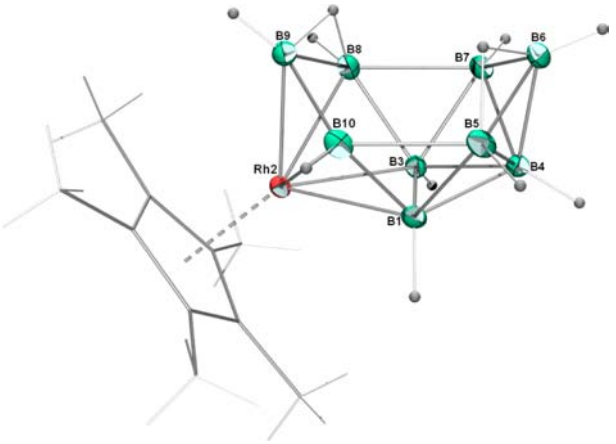

Figure 5. Molecular structure and labeling diagram for $[(Cp^*Rh)B_9H_{13}]$, **2**. Selected bond lengths (Å) and angles (deg): Rh1−B1 2.156(10), Rh1−B10 2.167(9), Rh1−B8 2.163(10), B1−B10 1.770(16), B5−B10 1.940(16), B3−B8 1.777(14), B3−B4 1.793(13), B4−B6 1.712(13), B6−B7 1.787(15); B9−Rh2−B10 51.8(5), B9−Rh2−B3 88.7(4), B6−B4−B5 61.3(6), B5−B4−B7 105.0(7), B1−B4−B3 61.3(6), B6−B4−B3 111.4(7).

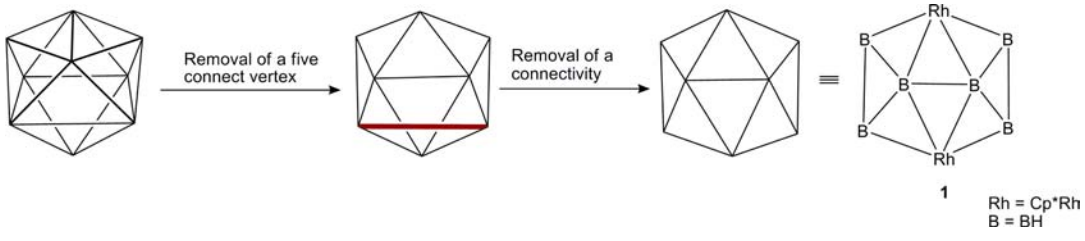

Figure 4. Schematic generation of the cluster framework of **1** from tricapped trigonal prism.

dx.doi.org/10.1021/ic301070e | *Inorg. Chem.* 2012, 51, 10715−10722

as having a total of 12 sep. The bridging hydrogens have not been positioned by X-ray diffraction studies; however, their connectivity have been assertively determined by ^{1}H NMR. The framework geometry of **2** is similar to that of $B_{10}H_{14}$ with a BH group replaced by an isolobal {Cp*Rh} fragment. A comparison with the established structures of $[(\eta^5\text{-}C_5H_5Co)B_9H_{13}]$,[19] 2- and 5-isomers of $[2\text{-THF-}6\text{-}(CO)_3\text{-}6\text{-}MnB_9H_{12}]$,[20] and 1- and 2-isomers of *nido*-$[(\eta^6\text{-}C_6Me_6)RuB_9H_{13}]$[21] suggests that the metal and its ligands are important in determining metal position and stability of a *nido* 10-atom cluster. In the case of Mn and Co analogues, the metals are at the open face, whereas in **2** the metal is having the highest connectivity.

$[(Cp^*Rh)_2B_8H_{12}]$, 3. The *nido* structure of **3**, shown in Figure 6, can be derived from an 11-vertex octadecahedron by

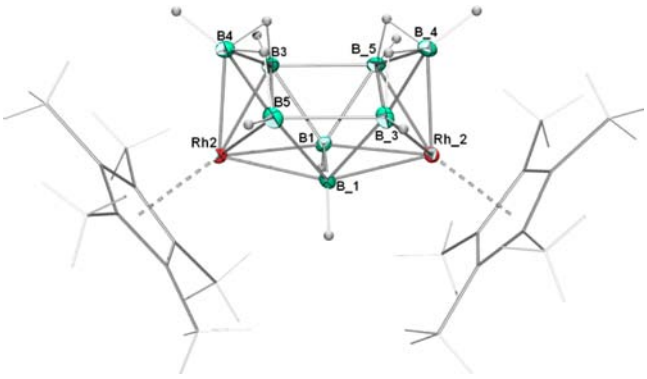

Figure 6. Molecular structure and labeling diagram for $[(Cp^*Rh)_2B_8H_{12}]$, **3**. Selected bond lengths (Å) and angles (deg): Rh2−B1 2.157(5), Rh2−B3 2.136(6), Rh2−B5 2.149(7), Rh2−B4 2.054(8), Rh2−B_1 2.164(5), B1−B_1 1.868(10), B1−B_5 1.781(10), B5−B4 1.850(13), B4−B3 1.854(11); B3−Rh2−B1 48.8(3), B4−Rh2−B3 52.5(3), B5−Rh2−B1 85.8(3), B5−Rh2−B_1 48.8(3), B3−B1−Rh_2 125.3(5), B3−B1−B_5 67.4(5).

the loss of the vertex of highest connectivity. The dimetallic species **3** has idealized C_{2v} symmetry, with a pseudo-mirror-plane through Rh1, B4, Rh_1, and B_4 and a second plane containing B1 and B_1, which is perpendicular to the first. The ^{11}B NMR of **3** further suggests a structure of higher symmetry than compound **2**. Consistent with our findings, **3** shows only one kind of Cp* signal and one kind of B−H−B proton indicating that the metal moieties as well as the bridging hydrogen atoms on the open faces are equivalent (Scheme 1). Analogous to **2**, the geometry of **3** can be described as the replacement of two boron vertices in decaborane, $[B_{10}H_{14}]$, by the isolobal {Cp*Rh} fragments.

Cluster **3** is a case of a polyhedral cluster, similar to 10 vertex boranes, carboranes, or metallaboranes having same skeletal electron pairs and geometry. Therefore, we have tried to contrast its structural data and chemical shifts values with a set of similar cluster types of formal electron counts of 12 sep, such as, $[(Cp^*Ir)_2B_8H_{12}]$,[11] 6,9-$[(Cp^*Co)_2B_8H_{12}]$,[22] 5,7-$[(Cp^*Co)_2B_8H_{12}]$,[22] $[B_{10}H_{14}]$,[23,24] and $[C_2B_8H_{12}]$.[25,26] The molecular structures of these clusters reveal that they have similar geometries and satisfy the electron counting rules derived from the borane analogy. Thus, the structure of **3** can be interpreted as a *nido* cluster formally derived from an 11-vertex *closo* octadecahedron.

$[(Cp^*Rh)_3B_8H_9(OH)_3]$, 4. The fourth metallaborane product **4** has been isolated as a minor product, and the ^{11}B NMR spectrum of **4** displays five resonances in the ratio of 2:2:1:2:1, distributed over an unusually large chemical shift range. Besides the BH terminal protons, two B−H−B and two Rh−H−B protons with an equal intensity were observed. The ^{1}H and ^{13}C NMR spectra imply two types of Cp* ligands in 2:1 ratio. The IR spectrum of **4** shows a band at 1345 cm^{-1} in a region characteristic of the B−O and a band at 3610 cm^{-1} that corresponds to O−H stretching frequency.

The framework structure of **4** became clear when a solid state structure was undertaken. The single crystal X-ray structure of **4**, shown in Figure 7, shows that three oxygen atoms are bound

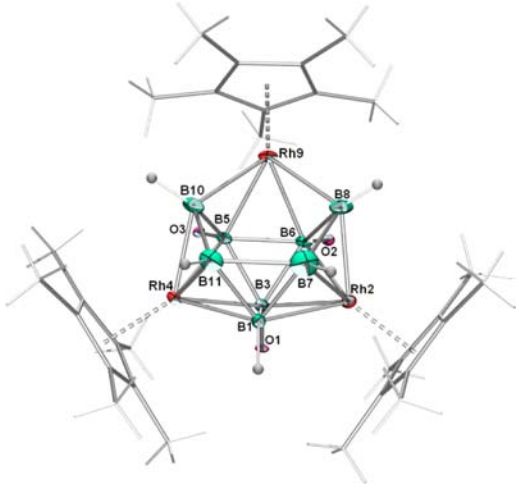

Figure 7. Molecular structure and labeling diagram for $[(Cp^*Rh)_3B_8H_9(OH)_3]$, **4**. Selected bond lengths (Å) and angles (deg): Rh2−B8 2.135(8), Rh2−B6 2.193(7), Rh2−B7 2.08(2), Rh4−B10 2.149(8), Rh4−B5 2.183(6), Rh9−B8 2.152(9), B8−B6 1.829(10), B10−B11 1.934(13), B5−B10 1.865(10); B1−Rh2−B8 96.2(4), B6−Rh2−B1 87.6(3), B5−Rh9−B10 49.8(3), B6−Rh9−B5 87.5(3), B1−Rh4−B11 51.7(3), B10−Rh4−B1 89.2(3).

to three boron atoms. Cluster **4** displays a shape that can be derived from a 12-vertex icosahedron by removing one of the apical vertices (Figure 8). Thus, it has *nido* geometry with prescribed 13 skeletal electron pair (sep). Alternatively, the observed geometry of **4** may be generated from an octadecahedron by the removal of two edges. Cluster **4** is comparable to those of 11 vertex metallacarborane and heterometallacarborane clusters, for example, [*nido*-7,8,9-$PC_2B_8H_{11}$],[27] [8,8-η^2-{η^2-(BH_3)·dppm}-*nido*-8,7-$RhSB_9H_{10}$],[28] [9,9-η^2-{η^2-(BH_3)·dppm}-*nido*-9,7,8-$RhC_2B_8H_{11}$],[28] $[(\mu\text{-}PPh_2)(PPh_3)_2Pt_2B_9H_6$ $(O^iPr)_3]$.[29] Even though we do not have any direct evidence for the presence of oxygen in **4**, it has previously been observed in other polyborane/$[\{Cp^*RhCl_2\}_2]$ systems when handled in air.[30−32] Therefore, the trace amount of water/air bound to the silica gel leads to the formation of **4**.

Metal Fragment Addition to *nido*-$[(Cp^*Rh)_2B_6H_{10}]$, 1. The cluster expansion reactions are now well-known;[33,34] however, high yield with clean and well-defined stoichiometry examples are limited. Availability of **1** and the resourcefulness of metal carbonyl compounds as important building block for cluster growth reaction tempted us to verify the reactivity of rhodaborane **1** with $[Fe_2(CO)_9]$. As shown in Scheme 2, a room temperature reaction of **1** with $[Fe_2(CO)_9]$ yielded a condensed product $[Fe_2(CO)_6(Cp^*Rh)_2B_6H_{10}]$, **5**. The IR spectrum in the carbonyl region shows terminal carbonyl frequencies at 2053, 2001, and 1938 cm^{-1}. Unlike **1**, cluster **5**

dx.doi.org/10.1021/ic301070e | *Inorg. Chem.* 2012, 51, 10715−10722

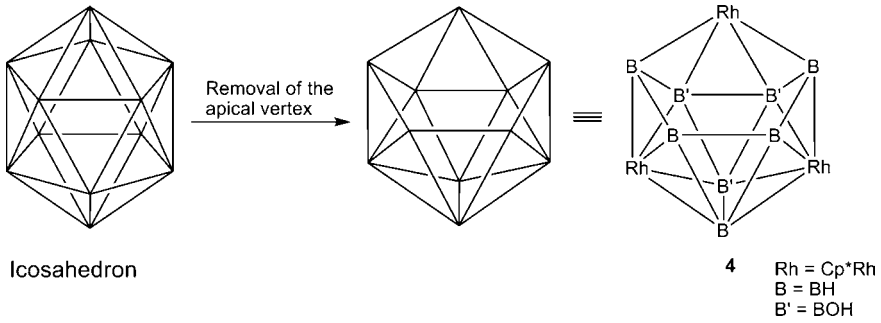

Figure 8. Generation of the observed geometry of **4** from an icosahedron by removing one of the apical vertices.

Scheme 2. Synthesis of Condensed Cluster 5

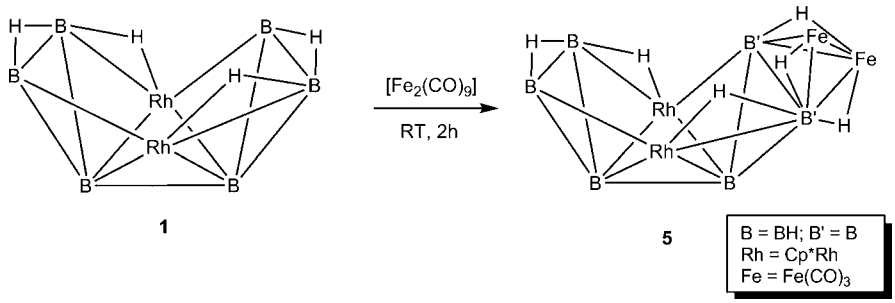

does not possess the plane of symmetry which is confirmed by ^{1}H and ^{11}B NMR spectra. Comparing the ^{1}H NMR with **1** the resonances at δ = −9.37, −9.97, and −11.95 ppm are assigned to three B−H−Fe protons, while the resonances at δ = −13.42 and −13.83 ppm are assigned to two B−H−Rh protons.

The constitution of **5** was established by an X-ray diffraction study on a suitable single crystal. Compound **5** displays a condensed structure (Figure 9) of rhodaborane $[(Cp^*Rh)_2B_6]$

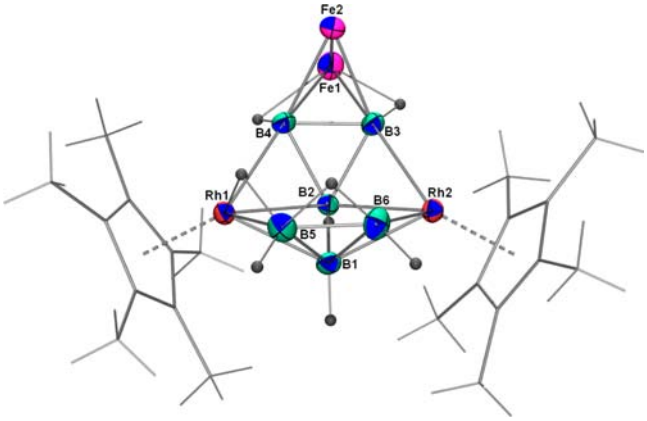

Figure 9. Molecular structure and labeling diagram for $[Fe_2(CO)_6(Cp^*Rh)_2B_6H_{10}]$ (**5**) (CO ligands are not shown for clarity). Relevant bond lengths (Å) and angles (deg): Rh1−B2 2.182(5), Rh1−B4 2.198(5), Rh1−B5 2.201(6), Rh2−B3 2.139(5), Rh2−B6 2.160(6), Rh2−B1 2.246(5), B2−B3 1.777(7), B2−B4 1.790(7), B2−B1 1.819(7), B1−B5 1.744(8), B1−B6 1.770(7), Fe1−B3 2.242(5), Fe1−Fe2 2.5795(10), Fe2−B3 2.099(5); B2−Rh1−B4 48.24(17), B2−Rh1−B5 85.34(19), B4−Rh1−B5 97.9(2), B3−Fe2−Fe1 56.14(13), B4−Fe2−Fe1 55.71(13).

core and an external $\{Fe_2B_2\}$ unit through two common boron atoms, which is similar to the ruthenium analogue, $[Fe_2(CO)_6(Cp^*RuCO)(Cp^*Ru)B_6H_{10}]$.[34]

It has been well established that a large number of condensed clusters can be described by the fusion of smaller cluster fragments.[1,35,36] According to Mingos approach,[37,38] the total electron count in such a condensed cluster is equal to the sum of the electron counts for the parent polyhedra minus the electron count of the shared unit(s) (atom, pair of atoms etc.). Therefore, as shown in eq 1, cluster **5** (cve=84) (cve = cluster

$$\begin{array}{lccc} & [(Cp^*Rh)_2B_6H_{10}] + [\,Fe_2(CO)_9] & & \\ \text{cve} & 56 \qquad\qquad 34 & & (1) \\ \longrightarrow & [Fe_2(CO)_6(Cp^*Rh)_2B_6H_{10}] + 3CO & & \\ & 84 \qquad\qquad 6 & & \end{array}$$

valence electrons) can be viewed as formed from the condensation of [*nido*-(η^5-$C_5Me_5Rh)_2B_6H_{10}$] (cve=56) and $[Fe_2(CO)_9]$ (cve=34) with elimination of three CO molecules (cve=6).

The mno rule[39] is also consistent with cluster **5**. Considering {Cp*Rh} as two electron fragment, the total skeletal electron count (sep) for **5** is 12. The mno rule also gives m = 2, n = 10, and o = 0 for $m + n + o$ = 12 (where m is the number of polyhedra, n the number of vertices in the fused cluster, and o the number of single vertex shared atoms).

CONCLUSION

A rational, useful synthetic route to rhodaboranes has been developed on the basis of the reactions of monoboranes with $[Cp^*RhCl_2]_2$. The structural properties of the clusters reported in this Article are interesting and obey electron-counting rules as well. Cluster **1** is the structurally characterized metallaborane analogue of $[B_8H_{12}]$ and is a new entry after $[(Cp^*Ru)_2B_6H_{12}]$. Although low temperature study of the parent molecule $[B_8H_{12}]$ was earlier performed by Sneddon,[40] the VT NMR performed on **1** sheds additional light into the dynamic behavior of the molecule and discloses the identity of two isomers. Further, it is exciting to see at what degree it might be likely to replace the

dx.doi.org/10.1021/ic301070e | Inorg. Chem. 2012, 51, 10715−10722

Table 1. Crystallographic Data and Structure Refinement Information for 1−5

	1	2	3	4	5
empirical formula	$C_{20}H_{38}B_6Rh_2$	$C_{10}H_{26}B_9Rh$	$C_{20}H_{42}B_8Rh_2$	$C_{66}H_{113}B_{15}O_6Rh_6$	$C_{26}H_{38}B_6Fe_2O_6Rh_2$
fw	549.18	347.52	574.84	1782.17	828.94
cryst syst	monoclinic	monoclinic	orthorhombic	triclinic	monoclinic
space group	$P2_1/n$	$P2_1/n$	$Fdd2$	P-1	$C2/c$
a (Å)	8.5186(4)	8.3821(3)	8.4472(2)	8.2493(4)	34.1297(15)
b (Å)	13.5052(7)	16.1918(6)	40.1716(10)	11.9167(5)	13.6561(7)
c (Å)	21.4987(11)	13.2597(6)	15.6305(4)	20.1796(10)	16.0775(8)
α (deg)	90	90	90	102.387(2)	90
β (deg)	91.407(2)	101.079(4)	90	90.134(2)	113.602(2)
γ (deg)	90	90	90	99.066(2)	90
V (Å^3)	2472.6(2)	1766.08(12)	5304.0(2)	1912.02(15)	6866.5(6)
Z	4	4	8	1	8
D_{calcd} (g/cm^3)	1.475	1.307	1.440	1.548	1.604
F (000)	1112	708	2336	902	3312
μ (mm^{-1})	1.338	0.947	1.250	1.311	1.808
cryst size (mm^3)	0.45 × 0.35 × 0.05	0.23 × 0.18 × 0.13	0.18 × 0.13 × 0.10	0.25 × 0.10 × 0.08	0.35 × 0.20 × 0.15
θ range (deg)	1.78−30.82	2.95−25.00	3.14−24.99	1.77−25.00	1.30−28.38
no. of total refins collected	18 721	13 648	8810	20 643	24 988
no. of unique refins [$I > 2\sigma(I)$]	6868	3098	2259	6424	8118
max and min transm	0.962 and 0.601	0.8868 and 0.8116	0.8852 and 0.8063	0.921 and 0.703	0.7732 and 0.5703
data/restraints/params	6868/8/294	3098/0/234	2259/1/164	6424/7/439	8118/0/421
GOF on F^2	1.068	1.166	1.103	1.012	1.062
final R indices [$I > 2\sigma(I)$]	R1 = 0.0515	R1 = 0.0570	R1 = 0.0302	R1 = 0.0440	R1 = 0.0425
	wR2 = 0.1250	wR2= 0.1911	wR2 = 0.0803	wR2 = 0.0929	wR2 = 0.1187
R indices (all data)	R1 = 0.1025	R1 = 0.0625	R1 = 0.0306	R1 = 0.0702	R1 = 0.0699
	wR2 = 0.1448	wR2 = 0.1956	wR2 = 0.0807	wR2 = 0.1043	wR2 = 0.1568
largest difference in peak and hole (e/Å^3)	1.725 and −1.040	1.332 and −0.725	0.896 and −0.269	0.747 and −0.694	1.427 and −0.674

BH units by {Cp*Rh} fragment or metal carbonyl fragments ({Fe(CO)$_3$} or {Co$_2$(CO)$_5$}) in B_8 or B_{10} cages and what would be the structural disparity from the parent molecules. Previously, a condensation reaction with [Fe$_2$(CO)$_9$] was observed in ruthenaborane and tungstaborane systems and more recently in rhodium system. Hence, not only does borane addition result in increased cluster boron element nuclearity but also cluster condensation can be considered as an additional viable pathway for increasing nuclearity in the cluster framework.

EXPERIMENTAL SECTION

General Procedures and Instrumentation. All the operations were conducted under an Ar/N$_2$ atmosphere using standard Schlenk techniques or glovebox. Solvents were distilled prior to use under argon. [Cp*RhCl$_2$]$_2$, [LiBH$_4$·THF], and [BH$_3$·THF] were used as received (Aldrich). The external reference [Bu$_4$N(B$_3$H$_8$)], for the ^{11}B NMR, was synthesized with the literature method.[41] Preparative thin-layer chromatography was performed with Merck 105554 TLC silica gel 60 F_{254}, layer thickness 250 μm on aluminum sheets (20 × 20 cm^2). NMR spectra were recorded on a 400 and 500 MHz Bruker FT-NMR spectrometer. Residual solvent protons were used as reference (δ, ppm, C_6D_6, 7.16), while a sealed tube containing [Bu$_4$N(B$_3$H$_8$)] in [D$_6$]benzene (δ_B, ppm, −30.07) was used as an external reference for the ^{11}B NMR. Microanalyses for C and H were performed on Perkin Elimer Instruments series II model 2400. Infrared spectra were recorded on a Thermo Nicolet iS10 FT spectrometer.

General Procedure for the Synthesis of 1−4. In a typical reaction, [Cp*RhCl$_2$]$_2$ (0.070 g, 0.113 mmol) was suspended in toluene (15 mL) and cooled to −78 °C, [LiBH$_4$·THF] (0.4 mL, 0.678 mmol) was added via syringe, and the reaction mixture was allowed to warm slowly to room temperature and left stirring for an additional hour. The solvent was evaporated under vacuum, the residue was extracted into hexane, and filtration afforded an extremely air- and moisture-sensitive red-orange intermediate. The filtrate was concentrated, and a toluene solution (15 mL) of the intermediate was thermolyzed at 105 °C with [BH$_3$·THF] (3.5 mL, 3.5 mmol) for 30 h. The solvent was dried, and the residue was extracted into hexane and passed through Celite. After removal of solvent, the residue was subjected to chromatographic work up using silica gel TLC plates. Elution with a hexane/CH_2Cl_2 (95:5 v/v) mixture yielded yellow **1** (0.013 g, 20%), colorless **2** (0.005 g, 12%), colorless **3** (0.02 g, 30%), purple **4** (0.003 g, 3%), and orange **I** (0.013 g, 15%).

Compound **I** has been characterized by comparison of its spectroscopic data reported earlier.[12]

Data for **1** follow. ^{11}B NMR (22 °C, 128 MHz, C_6D_6): δ 37.1 (d, J_{B-H} = 141 Hz, 4B), 5.3 (d, J_{B-H} = 133 Hz, 2B). ^{1}H NMR (22 °C, 400 MHz, C_6D_6): δ 6.1 (partially collapsed quartet (pcq), 4BHt), 2.3 (pcq, 2BHt), 1.82 (s, 30H; 2Cp*), −1.46 (br, 2 B−H−B), −14.1 (br, 2 Rh−H−B). ^{13}C NMR (22 °C, 100 MHz, C_6D_6): δ 101.27 ($C_5(CH_3)_5$), 9.5 ($C_5(CH_3)_5$). IR (hexane) ν/cm^{-1}: 2510w, 2498w (BHt). Anal. (%) Calcd for $C_{20}H_{40}B_6Rh_2$: C, 43.58; H, 7.31. Found: C, 43.39; H, 6.96.

Data for **2** follow. ^{11}B NMR (22 °C, 128 MHz, C_6D_6): δ 15.3 (d, J_{B-H} = 153 Hz, 2B), 10.7 (d, J_{B-H} = 159 Hz, 1B), 3.2 (d, J_{B-H} = 141 Hz, 1B), −1.5 (d, J_{B-H} = 154 Hz, 2B), −3.5 (d, J_{B-H} = 126 Hz, 2B), −41.9 (d, J_{B-H} = 166 Hz, 1B). ^{1}H NMR (22 °C, 400 MHz, C_6D_6): δ 4.12 (partially collapsed quartet (pcq), 1BHt), 3.8 (pcq, 2BHt), 3.1 (pcq, 2BHt), 2.3 (pcq, 2BHt), 1.62 (pcq, 1BHt), 1.12 (pcq, 1BHt), 1.91 (s, 15H; Cp*), −2.15 (br, 2B−H−B), −4.12 (br, 2B−H−B). ^{13}C NMR (22 °C, 100 MHz, C_6D_6): δ 104.05 ($C_5(CH_3)_5$), 9.48 ($C_5(CH_3)_5$). IR (hexane) ν/cm^{-1}: 2503w, 2448w (BHt). Anal. (%) Calcd for $C_{10}H_{28}B_9Rh_1$: C, 34.46; H, 8.10. Found: C, 34.19; H, 8.13.

Data for **3** follow. ^{11}B NMR (22 °C, 128 MHz, C_6D_6): δ 21.1 (d, J_{B-H} = 131 Hz, 2B), 9.4 (d, J_{B-H} = 161 Hz, 2B), 1.9 (d, J_{B-H} = 135 Hz, 4B). ^{1}H NMR (22 °C, 400 MHz, C_6D_6): δ 4.51 (partially collapsed quartet (pcq), 2BHt), 3.48 (pcq, 2BHt), 2.49 (pcq, 4BHt), 1.96 (s, 30H; 2Cp*), −3.52 (br, 4B−H−B) . ^{13}C NMR (22 °C, 100 MHz, C_6D_6): δ 101.87 ($C_5(CH_3)_5$), 9.60 ($C_5(CH_3)_5$). IR (hexane) ν/cm^{-1}: 2498w, 2453w (BHt). Anal. (%) Calcd for $C_{20}H_{42}B_8Rh_2$: C, 41.79; H, 7.36. Found: C, 41.49; H, 7.12.

dx.doi.org/10.1021/ic301070e | Inorg. Chem. 2012, 51, 10715−10722

Data for **4** follow. ^{11}B NMR (22 °C, 128 MHz, C_6D_6): δ 36.2 (s, 2B), 35.1 (d, J_{B-H} = 151 Hz, 2B), 21.9 (s, 1B), −0.8 (d, J_{B-H} = 136 Hz, 2B), −5.1 (d, J_{B-H} = 147 Hz, 1B). ^{1}H NMR (22 °C, 400 MHz, C_6D_6): δ 4.51 (partially collapsed quartet (pcq), 2BHt), 3.48 (pcq, 2BHt), 2.49 (pcq, 1BHt), 2.32 (s, 3H; 3OH), 1.89 (s, 15H; 1Cp*), 1.73 (s, 30H; 2Cp*), −3.52 (br, 2B−H−B), −14.31 (br, 2Rh−H−B). ^{13}C NMR (22 °C, 100 MHz, C_6D_6): δ 101.87 ($C_5(CH_3)_5$), 9.69 ($C_5(CH_3)_5$). IR (hexane) ν/cm^{-1}: 3610 (OH), 2506w, 2484w (BHt), 1345 (B−O).

Synthesis of 5. A yellow solution of compound **1** (0.06 g, 0.11 mmol) in hexane (15 mL) was stirred with 4 equiv of [$Fe_2(CO)_9$] (0.116 g, 0.44 mmol) at room temperature for 2 h. The solvent was removed in vacuo, and the residue was extracted in hexane and passed through Celite. The filtrate was concentrated and kept at −40 °C to remove [$Fe_3(CO)_{12}$]. The mother liquor was concentrated, and the residue was chromatographed on silica gel TLC plates. Elution with a hexane/CH_2Cl_2 (9:1) mixture yielded **5**, an air-stable reddish brown solid (0.056 g, 62%).

Data for **5** follow. ^{11}B NMR (22 °C, 128 MHz, C_6D_6): δ 34.7 (d, J_{B-H} = 140 Hz, 1B), 28.1 (d, J_{B-H} = 134 Hz, 1B), 25.2 (d, J_{B-H} = 153 Hz, 1B), 16.4 (s, 1B), 1.6 (d, J_{B-H} = 162 Hz, 1B), −12.3 (s, 1B). ^{1}H NMR (22 °C, 400 MHz, C_6D_6): δ 5.32 (partially collapsed quartet (pcq), 1BHt), 5.01 (pcq, 1BHt), 4.91 (pcq, 1BHt), 4.3 (pcq, 1BHt), 1.79 (s, 30H; 2Cp*), −1.83 (br, 1B−H−B), −9.37 (br, 1Fe−H−B), −9.97 (br, 1Fe−H−B), −11.95 (br, 1Fe−H−B), −13.42 (br, 1Rh−H−B), −13.83 (br, 1Rh−H−B). ^{13}C NMR (22 °C, 100 MHz, C_6D_6): δ 206.03 (CO), 101.8 ($C_5(CH_3)_5$), 9.63 ($C_5(CH_3)_5$). IR (hexane) ν/cm^{-1}: 2499w, 2473w (BHt), 2053s, 2001s, 1933s (CO). Anal. (%) Calcd for $C_{26}H_{40}B_6O_6Rh_2Fe_2$: C, 37.58; H, 4.85. Found: C, 37.34; H, 4.58.

X-ray Structure Determination. Crystallographic information for the compounds **1**−**5** is given in Table 1. The crystal data for **1**, **4**, and **5** were collected and integrated using a Bruker Axs Kappa Apex2 CCD diffractometer, with graphite monochromated Mo Kα (λ = 0.710 73 Å) radiation at 173 K. Crystal data for **2** and **3** were collected and integrated using Oxford Diffraction Xalibur-S CCD system equipped with graphite-monochromated Mo Kα radiation (λ = 0.71073 Å) at 150 K. The structures were solved by heavy atom methods using SHELXS-97[42] or SIR92[43] and refined using SHELXL-97 (G. M. Sheldrick, University of Göttingen).[44] Crystals suitable for X-ray diffraction studies were grown by cooling a concentrated hexane solution of **1**−**5** to −10 °C.

■ ASSOCIATED CONTENT

Ⓢ Supporting Information

Supplementary crystallographic data and X-ray crystallographic files for **1**-**5**. This material is available free of charge via the Internet at http://pubs.acs.org.

■ AUTHOR INFORMATION

Corresponding Author

*E-mail: sghosh@iitm.ac.in.

Notes

The authors declare no competing financial interest.

■ ACKNOWLEDGMENTS

Generous support of the Department of Science and Technology, DST (Project No. SR/SI/IC-13/2011), New Delhi is gratefully acknowledged. DKR thank the Council of Scientific and Industrial Research (CSIR), INDIA for Junior Research Fellowship. SKB and RSA also thank the University Grants Commission (UGC), INDIA, for Senior and a Junior Research Fellowship.

■ REFERENCES

(1) (a) Wade, K. *Electron Deficient Compounds*; Nelson: London, 1971. (b) Wade, K. *Adv. Inorg. Chem. Radiochem.* **1976**, *18*, 1−66.

(2) Mingos, D. M. P.; Wales, D. J. *Introduction to Cluster Chemistry*; Prentice Hall: New York, 1990.

(3) (a) Fehlner, T. P. *Organometallics* **2000**, *19*, 2643−2651. (b) Fehlner, T. P. *J. Chem. Soc., Dalton Trans.* **1998**, 1525−1532. (c) Fehlner, T. P. *Adv. Chem.* **2002**, *822*, 49−67.

(4) Roy, D. K.; Bose, S. K.; Geetharani, K.; Chakrahari, K. K. V.; Mobin, S. M.; Ghosh, S. *Chem.—Eur. J.* **2012**, *00*, 00.

(5) Bose, S. K.; Geetharani, K.; Varghese, B.; Mobin, S. M.; Ghosh, S. *Chem.—Eur. J.* **2008**, *14*, 9058−9064.

(6) (a) Aldridge, S.; Hashimoto, H.; Kawamura, K.; Shang, M.; Fehlner, T. P. *Inorg. Chem.* **1998**, *37*, 928−940. (b) Weller, A. S.; Fehlner, T. P. *Organometallics* **1999**, *18*, 447−450.

(7) Aldridge, S.; Shang, M.; Fehlner, T. P. *J. Am. Chem. Soc.* **1998**, *120*, 2586−2598.

(8) Weller, A. S.; Shang, M.; Fehlner, T. P. *Organometallics* **1999**, *18*, 53−64.

(9) Le Guennic, B.; Jiao, H.; Kahlal, S.; Saillard, J.-Y.; Halet, J.-F.; Ghosh, S.; Shang, M.; Beatty, A. M.; Rheingold, A. L.; Fehlner, T. P. *J. Am. Chem. Soc.* **2004**, *126*, 3203−3217.

(10) (a) Ghosh, S.; Beatty, A. M.; Fehlner, T. *Angew. Chem., Int. Ed.* **2003**, *42*, 4678−4680. (b) Ghosh, S.; Noll, B. C.; Fehlner, T. P. *Angew. Chem., Int. Ed.* **2005**, *44*, 2916−2918.

(11) Ghosh, S.; Noll, B. C.; Fehlner, T. P. *Dalton Trans.* **2008**, 371−378.

(12) Yan, H.; Beatty, A. M.; Fehlner, T. P. *Organometallics* **2002**, *21*, 5029−5037.

(13) Alvarez, A.; Macias, R.; Fabra, M. J.; Lahoz, F. J.; Oro, L. A. *J. Am. Chem. Soc.* **2008**, *130*, 2148−2149.

(14) Enrione, R.; Boer, F. P.; Limpscomb, W. *J. Am. Chem. Soc.* **1964**, *86*, 1451−1452.

(15) Gotcher, A. J.; Ditter, J. F.; Williams, R. E. *J. Am. Chem. Soc.* **1973**, 7514−7516.

(16) Lei, X.; Shang, M.; Fehlner, T. P. *J. Am. Chem. Soc.* **1998**, *120*, 2686−2687.

(17) Ho, J.; Deck, K. J.; Nishihara, Y.; Shang, M.; Fehlner, T. P. *J. Am. Chem. Soc.* **1995**, *117*, 10292−10299.

(18) Ghosh, S.; Lei, X.; Cahill, C. L.; Fehlner, T. P. *Angew. Chem., Int. Ed.* **2000**, *39*, 2900−2902.

(19) Wilcynski, R.; Sneddon, L. G. *Inorg. Chem.* **1979**, *18*, 864−866.

(20) Lott, J. W.; Gaines, D. F. *Inorg. Chem.* **1974**, *13*, 2261−2267.

(21) Bown, M.; Fontaine, L. R. X.; Greenwood, N. N.; Kennedy, D. J.; MacKinnon, P. *J. Chem. Soc., Chem. Commun.* **1987**, 817−818.

(22) Venable, T. L.; Sinn, E.; Grimes, R. N. *Inorg. Chem.* **1982**, *21*, 895−904.

(23) Kasper, J. S.; Lucht, C. M.; Harker, D. *Acta Crystallogr.* **1950**, *3*, 436−455.

(24) Eaton, R. G.; Lipscomb, W. N.; Benjamin, W. A. *NMR Studies of Boron Hydrides and Related Compounds*; W.A. Benjamin: New York, 1969.

(25) Šubrtova, V.; Linek, A.; Hašek, J. *Acta Crystallogr.* **1982**, *B38*, 3147−3149.

(26) Plešek, J.; Heřmánek, S. *Pure Appl. Chem.* **1974**, *39*, 431−454.

(27) Stibr, B.; Holub, J.; Bakardjiev, M.; Hnyk, D.; Tok, O. L.; Milius, W.; Wrackmeyer, B. *Eur. J. Inorg. Chem.* **2002**, 2320−2326.

(28) Volkov, O.; Macias, R.; Rath, N. P.; Barton, L. *Inorg. Chem.* **2002**, *41*, 5837−5843.

(29) Dou, J.; Wu, L.; Guo, Q.; Li, D.; Wang, D. *Eur. J. Inorg. Chem.* **2005**, 63−65.

(30) Ditzel, E. J.; Fontaine, X. L. R.; Fowkes, H.; Greenwood, N. N.; Kennedy, J. D.; MacKinnon, P.; Sisan, Z.; Thornton-Pett, M. *J. Chem. Soc., Chem. Commun.* **1990**, 1692−1694.

(31) Fontaine, X. L. R.; Fowkes, H.; Greenwood, N. N.; Kennedy, J. D.; Thornton-Pett, M. *J. Chem. Soc., Chem. Commun.* **1985**, 1722−1723.

(32) Sahoo, S.; Mobin, S. M.; Ghosh, S. *J. Organomet. Chem.* **2010**, *695*, 945−949.

(33) (a) Housecroft, C. E. *Boranes and Metalloboranes*; Ellis Horwood: Chichester, U.K., 1990. (b) In *The Chemistry of Metal Cluster Complexes*; Shriver, D. F., Kaesz, H. D., Adams, R. D., Ed.; VCH: New York, 1990.

(34) Ghosh, S.; Fehlner, T. P.; Noll, B. C. *Chem. Commun.* **2005**, 3080−3082.
(35) (a) Wade, K. *Inorg. Nucl. Chem. Lett.* **1972**, *8*, 559−562. (b) Wade, K. *Adv. Inorg. Chem. Radiochem.* **1976**, *18*, 67.
(36) Mingos, D. M. P. *Nature (London), Phys. Sci.* **1972**, *236*, 99.
(37) Mingos, D. M. P. *Acc. Chem. Res.* **1984**, *17*, 311−319.
(38) Mingos, D. M. P. *J. Chem. Soc., Chem. Commun.* **1983**, 706−708.
(39) Jemmis, E. D.; Balakrishnarajan, M. M.; Pancharatna, P. D. *J. Am. Chem. Soc.* **2001**, *123*, 4313−4323.
(40) Rietz, R. E.; Schaeffer, R.; Sneddon, L. G. *Inorg. Chem.* **1972**, *11*, 1242−1244.
(41) Ryschkewitsch, G. E.; Nainan, K. C. *Inorg. Synth.* **1974**, *15*, 113−114.
(42) Sheldrick, G. M. *SHELXS-97*; University of Göttingen: Gottingen, Germany, 1997.
(43) Altonare, A.; Cascarano, G.; Giacovazzo, C.; Guagliardi, A. *J. Appl. Crystallogr.* **1993**, *26*, 343−350.
(44) Sheldrick, G. M. *SHELXL-97*; University of Göttingen: Gottingen, Germany, 1997.